Rare Metal Materials and Engineering
Volume 52, Issue 10, October 2023
Available online at www.rmme.ac.cn

Science Press

Cite this article as: Liu Fei, Sun Wei, Wang Li, et al. Crystal Structure Prediction, Electronic Structure and Mechanical Properties of CrB: A First-Principles Investigation[J]. Rare Metal Materials and Engineering, 2023, 52(10): 3399-3409.

ARTICLE

Crystal Structure Prediction, Electronic Structure and Mechanical Properties of CrB: A First-Principles Investigation

Liu Fei, Sun Wei, Wang Li, Jia Bin

School of Materials Engineering, Tianjin Sino-German University of Applied Science, Tianjin 300350, China

Abstract: Different crystal structures of CrB were obtained by the CALYPSO software. The electronic structure and mechanical properties of CrB were analyzed through first-principles calculations. The results show that the structure of CrB transits from α-CrB to β-CrB phase when the pressure exceeds 90 GPa. The β-CrB phase exhibits both covalent and ionic bonds, while α-CrB phase is dominated by ionic bonds. The modulus and hardness of both phases increase with increasing pressure. However, the hardness of β-CrB is less than that of α-CrB, indicating that the comprehensive mechanical properties of CrB are optimized at 90 GPa. From the perspective of electronic structure, the reasons for the changes in the mechanical properties of CrB under different pressures were explained.

Key words: first principle method; crystal structure; CrB; electronic structure

Superhard materials are widely used in various industries and contribute to national defense and the national economy[1–5], such as oil and natural gas mining, aerospace, machinery, coal and mineral mining, geological prospecting, due to their higher hardness, higher elastic modulus, and better thermal conductivity. As the service conditions of superhard materials are severer, the requirements for their properties become higher and higher. Diamond is the hardest material known in nature, with a hardness of 60–120 GPa. But it easily reacts with iron in the process of use, which shortens its service life[6]. Therefore, the design of new hardness materials has become a research field with a high degree of attention. At present, the compounds formed by transition metal elements and light elements, such as N and B, provide more possibilities for the development of hard materials[1,7–9]. Transition metal atoms have a higher electron concentration, so they have higher bulk modulus. The addition of light elements can form strong hybridization with the d orbital electrons of transition metal atoms to form a quasi-covalent bond, which can greatly improve the shear modulus and achieve higher hardness.

Cr element is a peculiar magnetic element; the number of valence electrons in the outermost layer is $3d^5 4s^1$, thus it has a high valence electron density. When it is compressed, the valence electrons in the outer layer of Cr atoms have a strong ability to repel each other and high resistance to compression, so it has an extremely high bulk elastic modulus. Moreover, adding B and Cr atoms to form chromium-boron compounds will make them have higher hardness. The most fundamental factor determining the mechanical properties of materials is the crystal structures. Experiments have verified that there are a large number of crystal structures as known in the current phase diagram of boron-chromium compounds, such as Cr_2B, Cr_3B_5, CrB, Cr_3B_4, CrB_2, CrB_4 [10]. However, due to a large number of crystal structures in the system, the phase boundary between each structure is blurred, which brings certain difficulties to the synthesis of a single phase. At present, the crystal structure of CrB depends mainly on the research literature and related crystal databases. However, there are few reports on the crystal structure and mechanical properties of CrB under different pressures. Zhang et al[11] studied the crystal structure and electronic properties of CrB_4 at 0–100 GPa using the first-principles method. Therefore, this study aimed to study the crystal structures, electronic properties at pressures ranging from 0 to 150 GPa to understand its properties.

With the development of computational materials science, predicting the possible crystal structure of materials and

Received date: March 02, 2022
Foundation item: Tianjin Science and Technology Planning Project (22YDTPJC00160)
Corresponding author: Sun Wei, Ph. D., Professor, School of Materials Engineering, Tianjin Sino-German University of Applied Science, Tianjin 300350, P. R. China, Tel: 0086-20-28776680, E-mail: sunwei@tsguas.edu.cn

Copyright © 2023, Northwest Institute for Nonferrous Metal Research. Published by Science Press. All rights reserved.

theoretically designing the structure of materials have critical scientific significance in guiding experimental synthesis. Consequently, the effective combination of theoretical prediction methods and experimental methods will considerably reduce the cost of testing as well as the waste of resources[12–13]. At present, the CALYPSO software has become one of the mainstream structure search software in the world for its efficient and accurate crystal structure prediction[14–15]. Its reliability has been extensively verified, especially for structural prediction in the field of superhard materials. The determination of the ground state structure and the phase transition sequence of the structure in a high pressure range have high consistency with the experimental results[16–17].

In summary, based on the first principle method of density functional theory, the crystal structures of CrB were searched via CALYPSO software, and the electronic structure and mechanical properties of the searched structures under different pressures were analyzed and predicted.

1 Computation

The CALYPSO software, based on a particle swarm optimization algorithm, was used to search the structure of CrB with 1 to 8 formula units, and the pressure range was 0–150 GPa. In the search process, 30 generations were searched, and 30 structures were generated in each generation. A VASP software package was used to optimize the searched structures[18]. The relation between valence electrons and ionic solids was described by the generalized gradient approximation (GGA) of the Perdew-Burke-Ernzerhof (PBE) approach[18–19]. The supersoft pseudopotential was used to describe the interaction between the valence electron and the ionic substance. The valence electron of the Cr atom is $3d^5 4s^1$, and the valence electron of the B atom is $2s^2 2p^1$. Under normal circumstances, when $3d^5 4s^1$ is selected as the valence electron of Cr atom, most of the chemical properties of Cr can be determined. However, as the pressure increases, the inner electron orbitals are "crushed", and the corresponding inner electrons may be treated as valence electrons. Therefore, different pseudopotentials may be selected for calculation in this study. Related literatures[20] have divided the core states and valence states of Fe atoms under different pressures through first-principles calculation. Based on Ref. [20], by selecting different pseudopotentials, the binding energy of Cr crystal cell with body-centered cubic was calculated at the pressure of 150 GPa. Wherein, the pressures are applied to the supercell based on the original lattice constant. When $3d^5 4s^1$ and $3p^6 3d^5 4s^1$ of Cr atoms are selected as valence electrons, the binding energy of Cr crystal is −5.9616 and −5.9659 eV, respectively. The difference in binding energy is less than 0.01 eV, indicating that the 3p orbital has little effect on the calculation results in the range of 0–150 GPa. Therefore, the Cr-pv pseudopotential was chosen, which is recommended by the VASP software, for the following calculation. Similarly, by selecting B pseudopotential and B-h pseudopotential, the binding energy of B crystal cell was calculated, which contains 36 atoms with a space group R-3mH (No. 166)[21] at the pressure of 150 GPa, and the binding energies of B crystal cells are −5.91118 and −5.91236 eV, respectively. Therefore, the B pseudopotential was chosen, which is recommended by the VASP software for the following calculation.

The plane wave cutoff energy was 450 eV. The first Brillouin zone integration adopts the Monkhorst-Pack grid method[22], the grid spacing was 0.003 nm. In the geometric optimization process, the total energy change ultimately converges to 1×10^{-5} eV per atom and the force acting on an atom decreases to 0.1 eV/ nm per atom. Phonon spectrum of CrB crystals was calculated by the PHONOPY software based on the density functional perturbation theory (DFPT) via the supercell method. The supercells of the α-CrB and β-CrB were set to 2×2×2 and 3×3×3, respectively, and the corresponding K points adopt 3×3×3 and 4×4×5 grids, respectively. In the calculation of mechanical properties, the shear modulus, Young's modulus and bulk modulus were all calculated by the Voigt-Reuss-Hill average algorithm[23].

2 Results and Discussion

2.1 Crystal structure prediction

The CALYPSO software is employed to obtain the crystal structures of CrB at 0 K and 0–150 GPa. The lattice constants and atomic positions are optimized for the above searched 50 crystal structures with the lowest energy, thus the crystal structure with relatively low energy is determined as the stable crystal structure of CrB. The search results show that when searching one formula unit, two crystal structures with lower energy were consulted in 0–150 GPa. The space groups are Fm-3m (No. 225) and P4/mmm (No. 123), marked as α-CrB phase and β-CrB phase, respectively. When searching 2 to 8 formula units at 0–150 GPa, one crystal structure with lower energy is discovered with the space group Cmcm (No. 63), marked as γ-CrB phase.

The relationship between the energy and pressure of the crystal is determined according to the formula $G=H-TS$ (G is Gibbs free energy, T is temperature, and H is enthalpy). The enthalpy value can be used to represent the free energy at 0 K. Variation of the thermodynamic enthalpy for different crystal structures with pressure is displayed in Fig.1a.

It can be observed that at 0–150 GPa, γ-CrB with a space group of Cmcm has a lower enthalpy value, indicating that γ-CrB phase is relatively stable and does not undergo a phase change. For the α-CrB phase with the space group Fm-3m and the β-CrB phase with P4/mmm, since their enthalpy value is higher than that of γ-CrB phase, they may be metastable phases. It is noticeable that when the pressure is less than 90 GPa, α-CrB phase has a lower enthalpy value; if the pressure exceeds 90 GPa, β-CrB phase appears to have a lower enthalpy value. Therefore, CrB may undergo structural phase transition from α-CrB phase to β-CrB phase at 90 GPa. As related scholars have done a lot of research on the crystal structure and mechanical properties of γ-CrB phase[24–26], the present study mainly discusses the crystal structure, electronic structure and mechanical properties of α-CrB and β-CrB

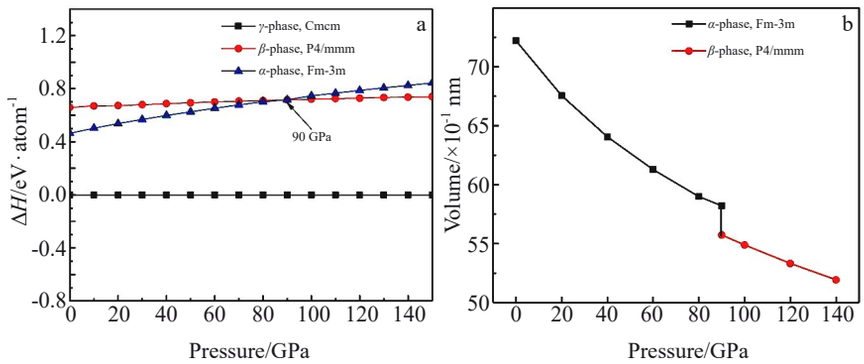

Fig.1 Variation of thermodynamic enthalpy (a) and volume changes (b) for different crystal structures of CrB with pressures

phases under different pressures.

Fig. 1b shows the volume changes of α-CrB and β-CrB phases with different pressures. The analysis demonstrates that the volume of the α-CrB phase decreases continuously with an increase in pressure. If the pressure reaches to 90 GPa, the structure of CrB undergoes a phase change to β-CrB, and its volume is decreased by about 4.25% compared with α-CrB.

Different crystal structures of CrB phase are shown in Fig.2. The optimized equilibrium lattice constants and atomic positions are listed in Table 1 and Table 2, respectively. Fig.2a shows the optimized crystal structure of α-CrB at 0 GPa. α-CrB phase has a cubic structure, and the lattice constant is a=b=c=0.416 nm. The Cr and B atoms in the crystal lattice are staggered in the [001], [010], and [100] crystal directions. The distance between each adjacent Cr and B atoms is 0.208 nm, and the distance between each adjacent Cr and Cr atoms, and B and B atoms is 0.294 nm. Fig. 2b shows the optimized crystal structure of β-CrB phase at 90 GPa. β-CrB phase has a tetragonal structure, and the lattice constants are a=b=0.254 nm, c=0.219 nm. Due to the higher pressure, the lattice constant is significantly smaller than that of α-CrB. In β-CrB phase, the Cr atoms and B atoms are clearly arranged in layers and stacked in the manner of ABAB. The distance between the Cr atomic layer and the B atomic layer is 0.219 nm. The distance between adjacent Cr atoms in the Cr atomic layer is equal to that of B atoms in the B atomic layer, both are 0.254 nm. Fig. 2c shows the optimized crystal structure of γ-CrB at 0 GPa. γ-CrB has orthogonal lattice with the space group

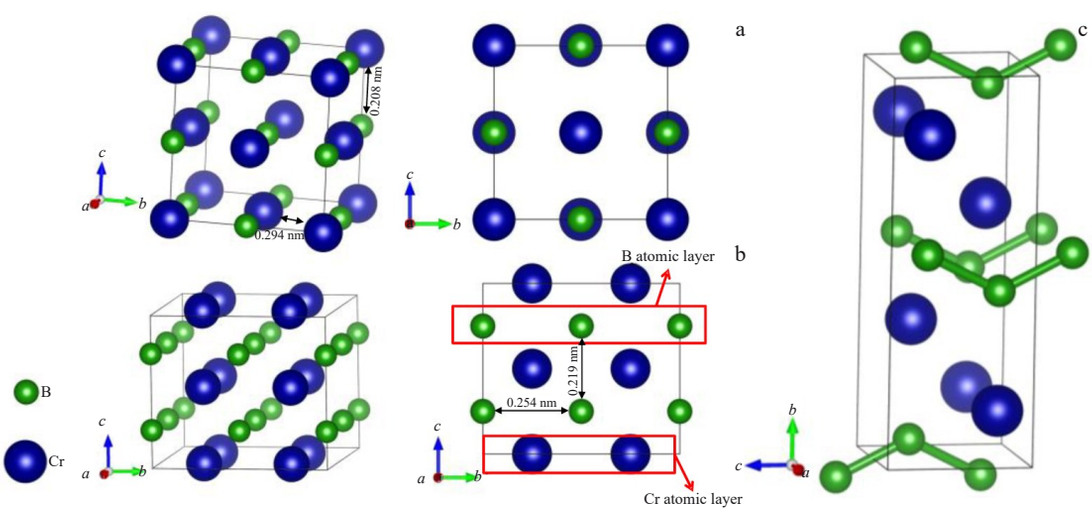

Fig.2 Crystal structures of CrB: (a) α-CrB phase at 0 GPa, (b) β-CrB phase at 90 GPa, and (c) γ-CrB phase at 0 GPa

Table 1 Optimized equilibrium lattice constants of CrB and atomic positions

Phase	Pressure/GPa	Source	a/×10^{-1} nm	b/×10^{-1} nm	c/×10^{-1} nm	α/(°)	β/(°)	γ/(°)
α-CrB (Fm-3m)	0	This work	4.16	4.16	4.16	90	90	90
β-CrB (P4/mmm)	90	This work	2.54	2.54	2.19	90	90	90
γ-CrB (Cmcm/mmm)	0	This work	2.91	2.91	7.85	90	90	90
γ-CrB (Cmcm/mmm)	0	Ref.[27]	2.92	2.91	7.84	90	90	90
γ-CrB (Cmcm/mmm)	0	Ref.[26]	2.97	2.93	7.86	90	90	90

Table 2 Optimized atomic positions of CrB

Phase	Pressure/GPa	Atom	Wyckoff position	*x*	*y*	*z*
α-CrB (Fm-3m)	0	Cr1	4*a*	0.5	0	0.5
		Cr2	4*a*	0.5	0.5	0
		Cr3	4*a*	0	0	0
		Cr4	4*a*	0	0.5	0.5
		B1	4*b*	0	0.5	0
		B2	4*b*	0	0	0.5
		B3	4*b*	0.5	0.5	0.5
		B4	4*b*	0.5	0	0
β-CrB (P4/mmm)	90	Cr1	1*c*	0.5	0.5	0
		B1	1*b*	0	0	0.5

Cmcm, which is composed of single boron layer and double Cr atom layers. It can be seen from Table 1 that the calculated lattice constant of the *γ*-CrB phase is in good agreement with the results in other literature, indicating that the calculation method used in this study is accurate.

2.2 Crystal structure stability

By calculating the phonon dispersion relationship, it can judge whether the lattice structure has dynamic stability. The condition for determining the dynamic stability of the lattice structure is that all normal phonon frequencies are finite real values[28]. If it is an imaginary value, it can judge that the structure has phonon softening and the lattice structure is unstable. In this work, the phonon spectrum of the predicted structure is calculated, as shown in Fig.3. It can be seen from Fig.3a that there is no phonon softening in the whole Brillouin zone of the *α*-CrB phase at 0 GPa, indicating that the phase has dynamic stability, and the frequency of the maximum optical branch is 20.70 THz. As can be seen from Fig.3b, at 90 GPa, the *β* -CrB phase has dynamic stability, and the maximum optical branch frequency is 22.35 THz. Therefore, although *α*-CrB phase and *β*-CrB phase are metastable phases, they both have dynamic stability.

2.3 Electronic structure analysis

To illustrate the predicted electronic structure of CrB, the band structures and electronic densities of states of *α*-CrB and *β*-CrB phase at 90 GPa are calculated, as shown in Fig. 4. It can be seen that the conduction band and the valence band of the two structures overlap near the Fermi surface, indicating that both structures are metallic. We clearly see from Fig. 4a that the electronic density of states in *α*-CrB phase is mainly contributed by the d orbital of Cr atom and the p orbital of B atom, whereas the energy range of the s orbital of Cr atom and B atom is smaller and the peak value of the density of states is low. Therefore, they have smaller contributions to the electronic density of states. In the energy range (eV) of [–4.42, –2.45], and [0.51, 1.92], and [4.03, 8.99], the d orbital of Cr atom and the p orbital of B atom have overlapping orbital energy distributions, indicating that the d orbital of Cr

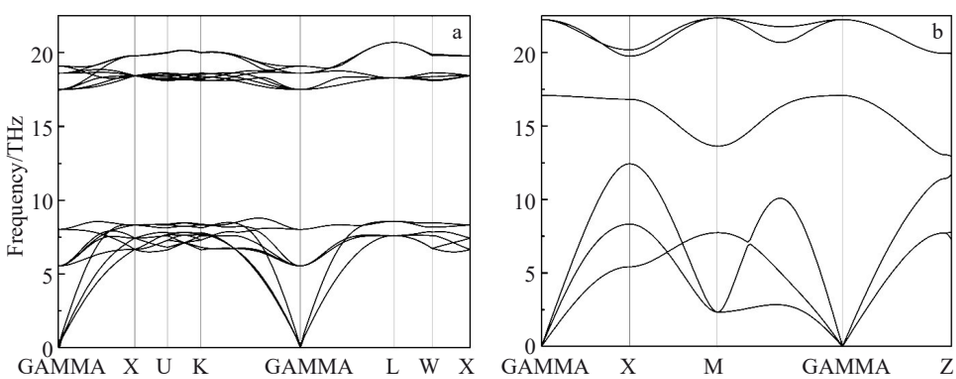

Fig.3 Phonon spectra of CrB: (a) *α*-CrB phase at 0 GPa and (b) *β*-CrB phase at 90 GPa

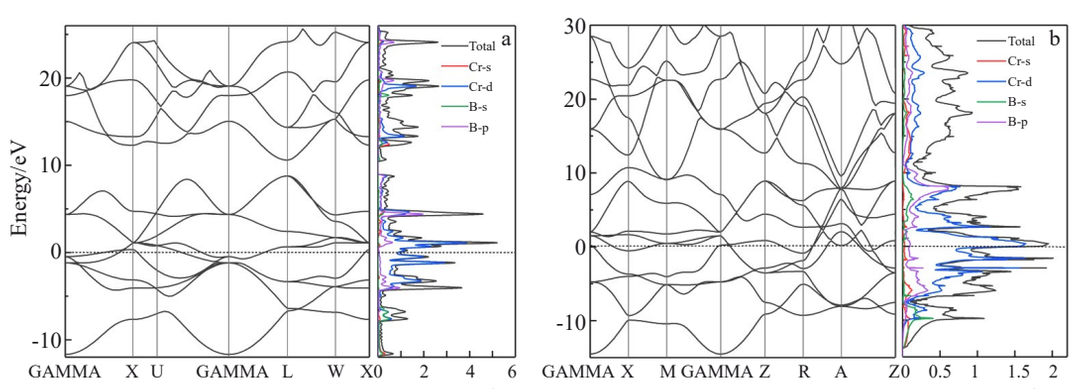

Fig.4 Band structures and partial density of states of CrB at 90 GPa: (a) *α*-CrB phase and (b) *β*-CrB phase

atom and the p orbital of B atom appear to be hybridized, and Cr atoms form bonds with B atoms. In the energy range (eV) of [– 6.18, – 7.92], there is an overlap in orbital energy distribution at the d orbital of Cr atom and the s orbital of B atom. Cr atoms and B atoms form bonds, but the bonding effect is relatively weak. Therefore, in the α-CrB phase, Cr atoms and B atoms form bonds, mainly due to the contributions of the d orbital of Cr and the p orbital of B. It can be seen from Fig.4b that the electronic density of states of the β-CrB phase is mainly contributed by the d orbital of Cr atom and the p orbital of B atom. The s orbital of B atom also has a certain contribution, but the contribution of s orbital of Cr atom is much smaller. In the entire energy range, the d orbital of Cr atom and the p orbital of B atom have overlapping orbital energy distributions, indicating that the d orbital of Cr atom and the p orbital of B atom appear to be hybridized, and Cr atoms form bonds with B atoms. In the energy range of 3.10–8.30 eV, the d orbital of Cr atom, p and s orbitals of B atom have overlapping orbital energy distributions, indicating that the d orbital of Cr atom, p and s orbitals of B atom appear to be hybridized, and Cr atoms form bonds with B atoms. Simultaneously, chemical bonds are formed between the B atoms. Compared with Fig. 4a and Fig.4b, the density of states energy range in the α-CrB phase is smaller and the peak value is higher, whereas the density of states energy range in the β-CrB phase is wider and the peak value is relatively low. It shows that the band dispersion in the β-CrB phase is strong, and thus the atomic orbital interaction is stronger.

In summary, the bonding effect of atoms in the β-CrB phase is stronger than in the α-CrB phase, which depends on the combined effect of the d orbital of Cr atom, p and s orbitals of B atom. Certainly, according to the results in Fig.1b, when the pressure exceeds 90 GPa, CrB undergoes a phase change, which reduces the volume of β-CrB phase, and the atomic distance is relatively close. Thus, it is the main reason for the strong bonding effect of atoms.

To illustrate the predicted electronic structure of CrB, the band structures and electronic densities of states of α-CrB and β-CrB phase at 90 GPa are calculated, as shown in Fig. 4. It can be seen that the conduction band and the valence band in the two structures overlap near the Fermi surface, indicating that both structures are metallic. We can clearly see from Fig. 4a that the electronic density of states in α-CrB phase is mainly contributed by the d orbital of Cr atom and the p orbital of B atom, whereas the energy range of the s orbital of Cr atom and the s orbital of B atom is smaller and the peak value of the density of states is low. Therefore, they have smaller contributions to the electronic density of states. In the energy (eV) range of [−4.42, −2.45], [0.51, 1.92], and [4.03, 8.99], the d orbital of Cr atom and the p orbital of B atom have overlapping orbital energy distributions, indicating that the d orbital of Cr atom and the p orbital of B atom appear to be hybridized, Cr atoms form bonds with B atoms. In the energy range from –6.18 eV to –7.92 eV, there is an overlap in orbital energy distribution at the d orbital of Cr atom and the s orbital of B atom. Cr atoms and B atoms form bonds, but the bonding effect is relatively weak. Therefore, in the α-CrB phase, Cr atoms and B atoms form bonds, mainly due to the contributions of the d orbital of Cr and the p orbital of B. It can be seen from Fig.4b that the electronic density of states of the β-CrB phase is mainly contributed by the d orbital of Cr atom and the p orbital of B atom. The s orbital of B atom also has a certain contribution, but the contribution of s orbital of Cr atom is much smaller. In the entire energy range, the d orbital of Cr atom and the p orbital of B atom have overlapping orbital energy distributions, indicating that the d orbital of Cr atom and the p orbital of B atom appear to be hybridized, Cr atoms form bonds with B atoms. In the energy range of 3.10 – 8.30 eV, the d orbital of Cr atom, p and s orbitals of B atom have overlapping orbital energy distributions, indicating that the d orbital of Cr atom, p and s orbitals of B atom appear to be hybridized, and Cr atoms form bonds with B atoms. Simultaneously, chemical bonds are formed between the B atoms. Compared with Fig. 4a and Fig. 4b, the density of states energy range in the α-CrB phase is smaller and the peak value is higher, whereas the density of states energy range in the β-CrB phase is wider and the peak value is relatively low. It shows that the band dispersion in the β-CrB phase is strong, and thus the atomic orbital interaction is stronger. In summary, the bonding effect of atoms in the β-CrB phase is stronger than that in the α-CrB phase, which depends on the combined effect of the d orbital of Cr atom, p and s orbitals of B atom. Certainly, according to the results in Fig. 1b, when the pressure exceeds to 90 GPa, CrB undergoes a phase change, which reduces the volume of β-CrB phase, and the atomic distance is relatively close. Thus, it is the main reason for the strong bonding effect of atoms.

To express the bonding types of atoms in different CrB structures more clearly, the differential charge density of α-CrB phase as well as β-CrB phase at 90 GPa is calculated, as shown in Fig.5.

Fig. 5a – 5c show the projections of differential charge density of α-CrB phase on the (001) plane, β-CrB phase on the (001) plane, and β-CrB phase on the (110) plane, respectively. The red area represents the electron-gained area, the blue area represents the electron-loss area, and green area represents the uniform electron gas. It can be seen from Fig.5a that electrons are obtained around B atoms in α-CrB phase, while lost around Cr atoms. This indicates that there is a strong charge

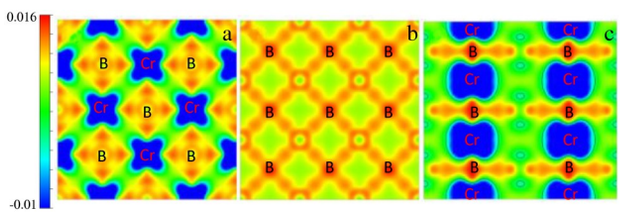

Fig.5 Differential charge density of the CrB phase: (a) α-CrB phase on the (001) plane, (b) β-CrB phase on the (001) plane, and (c) β-CrB phase on the (110) plane

transfer between Cr and B atoms, and Cr and B atoms form ionic bonds. In addition, there is no obvious charge effect between Cr and B atoms. It can be seen from Fig.5b that on the (001) plane of the β-CrB phase, that is, in the B atomic layer, electrons are obtained among all B atoms, and the electron clouds overlap each other, which indicates that there are sharing charge among B atoms, and a network of covalent bonds is formed among B atoms. The result of the density of binding states is easily concluded, i.e. the s and p orbitals of the B atom are hybridized, and covalent bonds are formed among B atoms. It can be seen from Fig.5c that on the (110) plane of the β-CrB phase, electrons are obtained around B atoms, while lost around Cr atoms. It indicates that there is a strong charge transfer between Cr and B atoms, and Cr and B atoms form ionic bonds. Therefore, combined with the analysis results of the density of states, it can be concluded that in the β-CrB phase crystal, the s and p orbitals of the B atoms in the B atomic layer are hybridized to form a covalent bond network, and hybridize with the d orbitals of the Cr atoms in Cr atomic layer, forming ionic bonds. The hybridization of these three atomic orbitals to form covalent bonds and ionic bonds is the main way of bonding among atoms in the β-CrB phase.

2.4 Mechanical properties analysis

The mechanical properties of the α-CrB phase and β-CrB phase (bulk modulus B, shear modulus G, Young's modulus E) can be calculated based on the obtained elastic constants. Voigt-Reuss-Hill is the best method to estimate the mechanical properties of crystals from elastic constants.

$$B = \frac{1}{2}(B_V + B_R) = \frac{1}{3}(C_{11} + 2C_{12}) \tag{1}$$

$$G_V = \frac{1}{5}(C_{11} - C_{12} + 3C_{44})$$
$$G_R = 5(C_{11} - C_{12})C_{44}/(4C_{44} + 3(C_{11} - C_{12})) \tag{2}$$

$$G = \frac{1}{2}(G_v + G_R);\ E = 9BG/(3B + G) \tag{3}$$

$$M = (C_{11} + C_{12} + 2C_{33} - 4C_{13}$$
$$C^2 = (C_{11} + C_{12})C_{33} - 2Ck_{13}{}^2 \tag{4}$$

$$G_V = \frac{1}{30}(M + (C_{11}M + 3C_{11} - 3C_{12} + 12C_{44} + 6C_{66})$$
$$B_V = \frac{1}{9}(2C_{11} + 2C_{12} + C_{33} + 4C_{13}) \tag{5}$$

$$G_R = 15[18B_v/C^2 + 6/(C_{11} - C_{12}) + 6/C_{44} + 3/C_{66}]^{-1}$$
$$B_R = C^2/M \tag{6}$$

$$B = \frac{1}{2}(B_v + B_R);\ G = \frac{1}{2}(G_v + G_R) \tag{7}$$

$$E = 9BG/(3B + G) \tag{8}$$

Since the α-CrB phase has a cubic structure, its elastic constant has only three independent variables, that is, C_{11}, C_{12}, and C_{44}. The mechanical properties of α-CrB phase can be calculated according to Eq.(1–3)[29].

The β-CrB phase has a tetragonal structure, and its elastic constants have six independent variables, that is, C_{11}, C_{12}, C_{13}, C_{33}, C_{44} and C_{66}. The corresponding mechanical properties are calculated according to Eq.(4–8)[29].

B_V, B_R, and B are the bulk moduli obtained by Voigt, Reuss and Voigt-Reuss-Hill, respectively, and G_V, G_R and G are the shear moduli obtained by Voigt, Reuss and Voigt-Reuss-Hill, respectively. In order to illustrate the accuracy of the calculation results, the author also calculated the elastic constants of the γ-CrB phase at 0 GPa, and then compared them with related literature[28]. The criterion of mechanical stability of cubic crystal systems is shown in Eq.(9), and the criterion of mechanical stability of tetragonal crystal system is shown in Eq.(10). The calculation results are shown in Table 3.

$$C_{11} > 0;\ C_{44} > 0;\ C_{11} - C_{44} > 0;\ C_{11} + 2C_{12} > 0 \tag{9}$$

$$(C_{11} - C_{12}) > 0;\ (C_{11} + C_{33} - 2C_{13}) > 0$$
$$C_{ii} > 0\ (i = 1, 3, 4, 6) \tag{10}$$

The elastic constant of the γ-CrB phase is in good agreement with the literature values, indicating that the calculated results of this study are more accurate. Substituting the data in Table 3 into Eq.(9) and Eq.(10), it was con-cluded that both the α-CrB phase and β-CrB phase satisfy the criterion of mechanical stability, indicating that both the α-CrB phase and β-CrB phase are mechanically stable.

From Table 3, obviously, $C_{11} < C_{33}$ for β-CrB. Generally, C_{11} and C_{33} can be used to describe the resistances to linear compression along the [100] and [001] directions, respectively. A high value of C_{11} and C_{33} indicates a large resistance to linear compression along the [100] and [001] direction[33]. Thereby, for β-CrB, the resistance to linear compression along the [100] direction is larger than that along the [001] direction. This is due to the fact that the strong bonds are parallel to the (001) plane while the weak bonds are perpendicular to the (001) plane or parallel to the (110) plane. Combining the results of electronic structure analysis in Fig.5b and Fig.5c, for β-CrB, covalent bonds network is formed among B atoms on the (001) crystal plane, while ionic bonds form among Cr atoms and the B atoms on the (110) crystal plane. Obviously,

Table 3 Calculated elastic constants of CrB

Phase	Pressure/GPa	Source	C_{11}/GPa	C_{12}/GPa	C_{13}/GPa	C_{22}/GPa	C_{23}/GPa	C_{33}/GPa	C_{44}/GPa	C_{55}/GPa	C_{66}/GPa
α-CrB	0		579.1	104.7					93.1		
β-CrB	90		754.6	521.8	410.4			902.8	254.1		455.5
γ-CrB	0		512.3	176.1	177.5	612.7	161.8	606.9	262.8	275.2	236.5
		Ref.[30]	503.5	182.8	159.3	588.2	158.9	586.8	237.1	272.6	219.2
		Ref.[31]	507.9	176.1	174.5	601.2	160.6	616.3	230.4	276.3	226.0
		Ref.[32]	505	170	166	604	147	613	233	278	225

the strong bonds are parallel to the (001) plane while the weak bonds are parallel to the (110) plane. This well explains the reason for C_{11}<C_{33} from the perspective of electronic structure.

Fig.6 shows the curves that reflect the change of the elastic constants and the elastic moduli of CrB with pressures. The values of elastic moduli are listed in Table 4. It can be seen from Fig.6a that the elastic constants of α-CrB and β-CrB both increase when pressure increases. The C_{11} value of α-CrB has a significant increasing trend, inferring that pressure is more likely to affect the electron bonding of α-CrB phase in the direction of [100].

When the pressure exceeds 90 GPa to form a phase change, the elastic constant of β-CrB phase changes significantly. The value of C_{11} decreases from 1287.4 GPa to 754.6 GPa, while C_{12} increases from 165.9 GPa to 521.8 GPa. The change of elastic constants directly affects the elastic modulus of CrB, as shown in Fig. 6b. B value mainly reflects the material's resistance to compression. The larger the value, the stronger the compression resistance. The value of E and G mainly reflects the material's stiffness. The larger value means that the material has stronger stiffness. The bulk modulus B, shear modulus G, and Young's modulus E of both α-CrB and β-CrB phases increase with an increase in pressure. When the pressure exceeds 90 GPa to form a phase change, the elastic modulus of β-CrB phase changes significantly. The bulk modulus B value increases significantly from 533.0 GPa to 969.2 GPa, while the shear modulus G decreases from 305.2 GPa to 242.6 GPa, Young's modulus E decreases from 769.0 GPa to 671.8 GPa. It can be said that when the pressure exceeds 90 GPa to form a phase change, the compression resistance of the CrB phase is greatly increased, whereas the stiffness is slightly reduced.

Fig. 7 shows the hardness and B/G values of CrB phase calculated under different pressures. Vickers hardness is calculated according to Eq.(11), where k=G/B.

$$H_v = 0.92k^{1.137}G^{0.708} \quad (11)$$

With an increase in pressure, the hardness of α-CrB phase gradually increases, reaching the maximum value of 28 GPa at 90 GPa. When the pressure exceeds 90 GPa, the hardness of the β-CrB phase decreases significantly, as low as 9.3 GPa.

With an increase in pressure, the volume incompressibility of the material increases, so the bulk modulus of the material increases. This can be clearly seen from Fig.6b. From Eq.(11), The increase in bulk modulus will reduce the hardness of the material, while increasing shear modulus will increase the hardness of the material. It can be seen from Fig.6b, when the pressure is lower than 90 GPa, with an increase in pressure, the shear modulus and bulk modulus increase at the same time, which eventually increase the hardness of the material. When the pressure exceeds 90 GPa and the phase transition occurs, the shear modulus of β phase decreases, which is the main reason for the decrease in hardness of β-CrB phase.

The reason for the change of the elastic modulus and hardness of CrB during the phase change will be discussed in Section 2.6 in conjunction with the analysis of the electronic structures.

Toughness and brittleness are important characteristics of material mechanical properties. In general, the natural

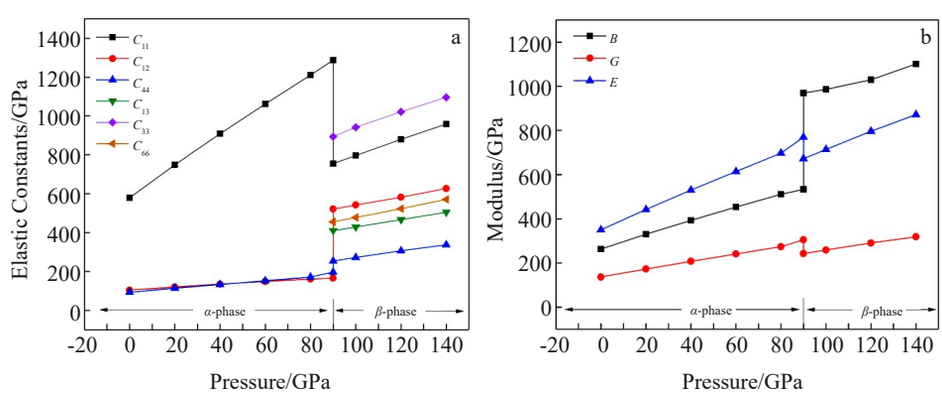

Fig.6 Curves reflecting the change of the elastic constants (a) and the elastic modulus (b) of CrB under different pressures

Table 4 Elastic modulus values of CrB

Phase	α-CrB						β-CrB			
Pressure/GPa	0	20	40	60	80	90	90	100	120	140
B/GPa	262.9	330.0	393.3	453.2	510.8	533.0	969.2	985.5	1029.1	1100.4
G/GPa	136.9	173.0	207.6	241.0	273.8	305.2	242.6	258.7	290.4	318.6
E/GPa	349.8	441.8	529.8	614.2	697.0	769.0	671.8	713.8	796.4	871.8
v	0.272	0.288	0.301	0.309	0.316	0.318	0.925	0.733	0.357	0.891
C_{12}–C_{44}/GPa	3.7	28.8	48.2	71.1	93.9	105.1				
C_{13}–C_{44}/GPa							213.3	222.8	396.1	264.9
B/G	1.92	1.90	1.89	1.88	1.86	1.75	3.99	3.81	3.54	3.45

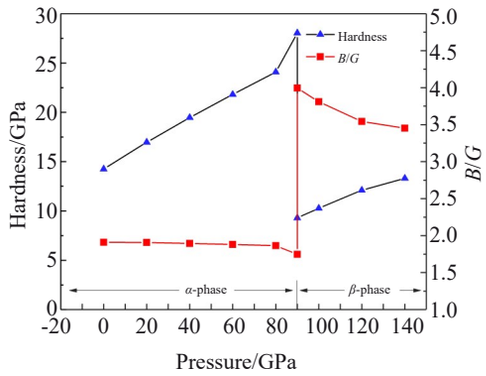

Fig.7 Hardness and B/G values of CrB phase calculated under different pressures

ductility and brittleness are predicted by Poisson's ratio[34], Paugh's ratio B/G[35], and the Cauchy pressure. Cauchy pressures are $C_{12}-C_{44}$ for cubic α-CrB and $C_{13}-C_{44}$ for tetragonal β-CrB. The solid appears to be brittle when ν<0.26, B/G<1.75 and Cauchy pressure<0; otherwise, it is ductile. From Table 4, ν, B/G and Cauchy pressures for both α-CrB and β-CrB meet the ductile requirements of ν>0.26, B/G>1.75 and $(C_{12}-C_{44})$ or $(C_{13}-C_{44})$>0, thereby suggesting that both α-CrB and β-CrB appear to be ductile at different pressures. From Fig. 7, as the pressure increases, B/G value of α-CrB phase decreases slightly, from 1.91 to 1.75. It can be explained by the fact that when the pressure reaches 90 GPa, α-CrB phase has the highest hardness; meanwhile the matching degree of toughness and hardness is the best. That is, the comprehensive mechanical properties of the material are the best in this state. When the pressure exceeds 90 GPa to form a phase change, the B/G value of β-CrB phase increases to 3.9, and the hardness of the material is as low as 9.3 GPa, showing an obvious characteristic of ductility.

2.5 Mechanical anisotropy

For hardness materials, the elastic anisotropy of materials is an important mechanical property. According to Eq. (9), the hardness of CrB depends mainly on the value of shear modulus G and bulk modulus B. Therefore, the anisotropy of the shear modulus and bulk modulus of CrB at 90 GPa was calculated. Based on the single crystal's elastic constant C_{ij} and its inverse matrix elastic flexibility coefficient S_{ij}, the bulk modulus and shear modulus anisotropies of α-CrB and β-CrB phases are characterized. Since the stress and strain of the shear modulus are perpendicular to each other and are not on the same plane, it is difficult to make a true three-dimensional figure. Therefore, the three-dimensional anisotropy of the torsional modulus (G_T) is used to approximate the shear modulus. For the cubic structure of α-CrB phase, the anisotropy of bulk modulus and shear modulus are calculated according to Eq. (12) and Eq. (13)[36]. For β-CrB phase with tetragonal structure, the anisotropy of bulk modulus and shear modulus is calculated according to Eq.(14) and Eq.(15).

$$1/B=(S_{11}+2S_{12})(l_1^2+l_2^2)+(S_{12}+2S_{11})l_3^2 \quad (12)$$

$$1/G_T=S_{11}+4S_{44}((S_{11}-S_{12})-0.5)(l_1^2l_2^2+l_1^2l_3^2+l_2^2l_3^2) \quad (13)$$

$$1/B=(S_{11}+S_{12}+S_{13})(l_1^2+l_2^2)+(2S_{11}+2S_{13})l_3^2 \quad (14)$$

$$1/G_T=2S_{11}l_1^2(1-l_1^2)+2S_{11}l_2^2(1-l_2^2)+2S_{33}l_3^2(1-l_3^2)-4S_{12}l_1^2l_2^2-4S_{13}l_1^2l_3^2-4S_{13}l_2^2l_3^2+0.5S_{44}(2-l_1^2-l_2^2-4l_2^2l_3^2-4l_1^2l_3^2)+0.5S_{66}(1-l_3^2-4l_1^2l_2^2) \quad (15)$$

where S_{ij} is the elastic compliance matrix, l_1, l_2, and l_3 are the direction cosines. The adoption of the relationship of the direction cosines in spherical coordinates with respect to θ and φ yields l_1=sinθcosφ, l_2=sinθsinφ, and l_3=cosφ. The calculated surface contours and anisotropic properties of bulk modulus and shear modulus are shown in Fig.8 and Fig.9.

Fig. 8 shows the anisotropic surface contours and projections of shear modulus of α-CrB and β-CrB at 90 GPa. An important factor that determines the hardness of a material is the ability to resist shear deformation. The maximum and minimum shear modulus of α-CrB phase is 296.9 and 196.8 GPa, respectively, G_{max}/G_{min}=1.51. The maximum and minimum shear modulus of β-CrB phase is 326.1 and 224.7 GPa, respectively, G_{max}/G_{min}=1.58. The shear modulus' anisotropy of β-CrB phase is not much different from that of α-CrB phase.

Fig.9 shows the surface contours and anisotropic properties of bulk modulus of α-CrB and β-CrB at 90 GPa. The maximum and minimum bulk modulus of α-CrB phase is 1602.2 and 662.8 GPa, respectively, B_{max}/B_{min}=2.42. The maximum and minimum bulk modulus of β-CrB phase is 4479.3 and 1358.8 GPa, respectively, B_{max}/B_{min}=3.30. The shear modulus' anisotropy of β-CrB phase is not much different from that of α-CrB phase. The anisotropy of bulk modulus of β-CrB is stronger than that of α-CrB phase.

2.6 Discussions

On the one hand, the most fundamental reason that determines the mechanical properties of materials is the strength of the internal atomic bonding of the materials; on the other hand, it is the crystal structures. The calculated results show that when the pressure exceeds 90 GPa, CrB will undergo a structural phase change, from α-CrB phase to β-CrB phase. At this time, the volume of β-CrB phase is reduced, that is, the distance between atoms is closer, which leads to a stronger interaction force between atoms in the β-CrB phase. From the perspective of electronic structure, this is mainly manifested in two aspects. (1) In β-CrB phase, the s and p orbitals of the B atoms in B atomic layer hybridize to form a covalent bond network and hybridize with the d orbitals of the Cr atoms in Cr atomic layer to form ionic bonds. These three atomic orbitals are hybridized, forming covalent bonds and ionic bonds. In α-CrB phase, the d orbital of Cr and p orbital of B are hybridized, and the Cr atoms and the B atoms only form ionic bonds. (2) The density of states energy range in the α-CrB phase is smaller and the peak value is higher, while the density of states energy range in the β-CrB phase is wider and the peak value is relatively low. The band dispersion in the β-CrB phase is strong, and thus the atomic orbital interaction is stronger.

Therefore, the stronger interaction of atoms in the β-CrB phase will result in excellent mechanical properties of the

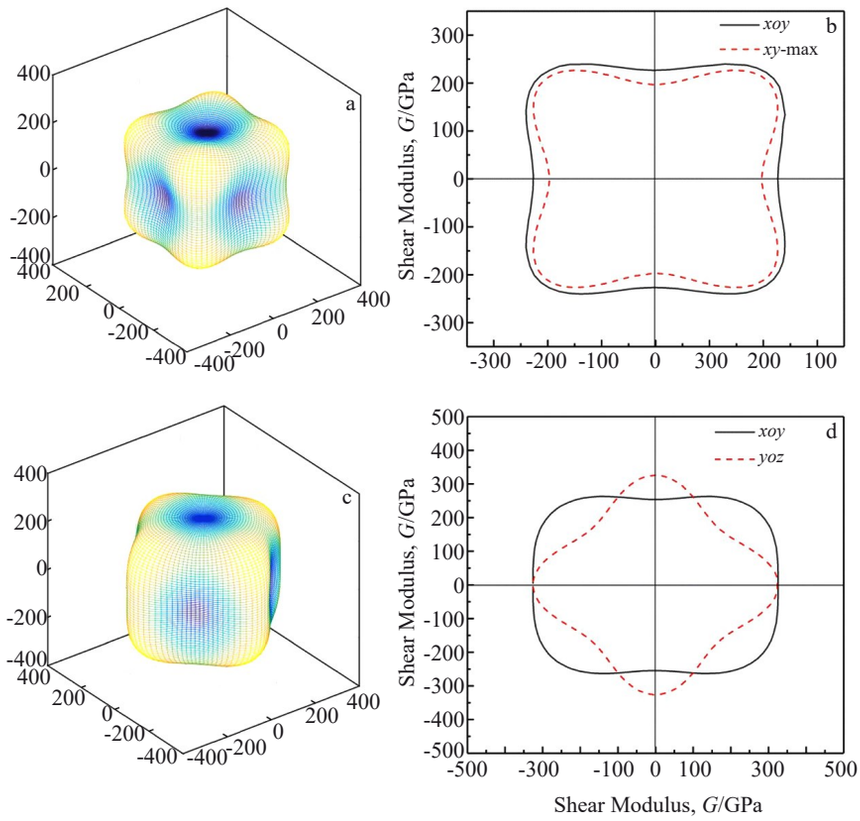

Fig.8 Anisotropic surface contours and projections of shear modulus G of the CrB phase at 90 GPa: (a) surface contours of α-CrB, (b) projection of α-CrB, (c) surface contours of β-CrB, and (d) projection of β-CrB

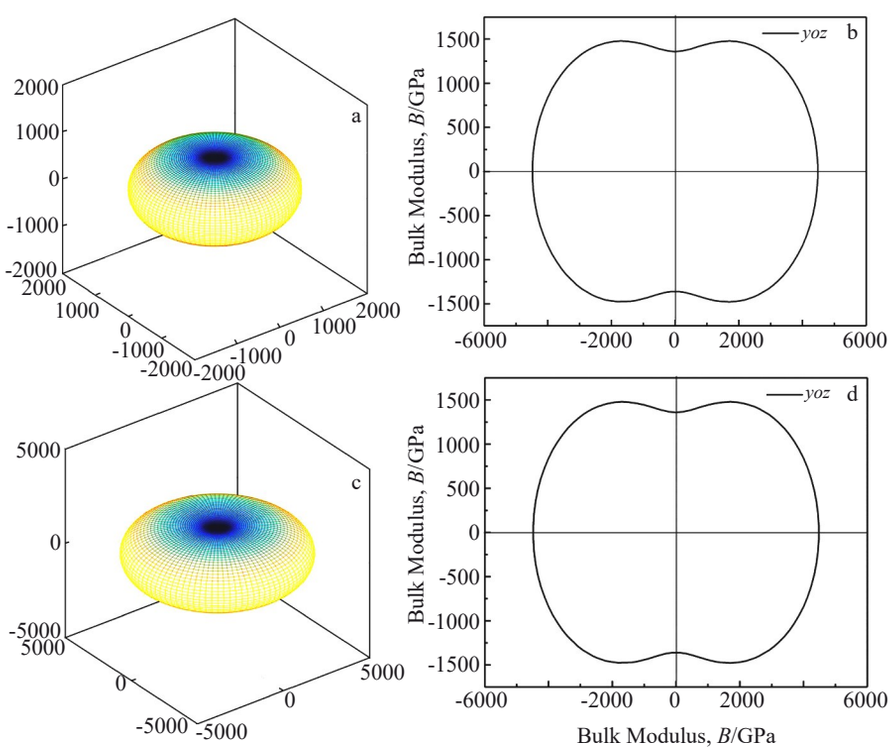

Fig.9 Anisotropic surface contours and projections of bulk modulus B of the CrB phase at 90 GPa: (a) surface contours of α-CrB, (b) projection of α-CrB, (c) surface contours of β-CrB, and (d) projection of β-CrB

crystal. It is not difficult to see from the calculation results of the mechanical properties that after the phase change, the bulk modulus of the β-CrB phase reaches to 969.2 GPa, which is much higher than that of α-CrB phase, indicating that the volume of the β-CrB crystals has greater incompressibility. However, it is not difficult to find that the shear modulus and Young's modulus of β-CrB phase are lower than those of α-CrB phase. This depends on the crystal structures of the α-CrB and β-CrB phase. The α-CrB phase crystal has a cubic structure, in which Cr and B atoms are staggered in the [001], [010], and [100] crystal directions, and form a chemical bond network with each other. While β-CrB phase has a tetragonal structure, in which Cr and B atoms are clearly arranged in layers and stacked in the manner of ABAB. In this way, in the β-CrB phase, covalent bonds network are formed among B atoms on the (001) crystal plane, and on the (110) crystal plane perpendicular to it, ionic bonds are formed among Cr atoms and the B atoms.

Combining the above analysis, it can be concluded that, when a phase change occurs, compared with β-CrB phase, α-CrB phase has lower interatomic force and smaller bulk modulus. But in the crystal structure, the formation of chemical bonds network among atoms reduces the anisotropy of the bulk modulus, so α-CrB phase has relatively high hardness and better comprehensive mechanical properties at 90 GPa.

3 Conclusions

1) Two structures of CrB are searched by one formula unit. α-CrB phase has a cubic structure with a space group Fm-3m (No. 225), in which Cr and B atoms are staggered in the [001], [010], and [100] crystal directions. β-CrB phase has a tetragonal structure with a space group P4/mmm (No. 123), in which Cr and B atoms are clearly arranged in layers and stacked in the manner of ABAB. When the pressure exceeds 90 GPa, CrB will undergo a structural phase change, from α-CrB phase to β-CrB phase.

2) The analysis result of the electronic structure shows that at 90 GPa, in β-CrB phase, the s and p orbitals of the B atoms in the B atomic layer are hybridized to form covalent bonds network and hybridize with the d orbitals of the Cr atoms in Cr atomic layer, forming ionic bonds. The hybridization of these three atomic orbitals to form covalent bonds and ionic bonds is the main way of bonding among atoms in β-CrB phase. In α-CrB phase, the d orbital of Cr atom and the p orbital of B atom hybridize, and Cr atoms form bonds with B atoms.

3) The calculated results of mechanical properties show that when pressure increases, the hardness of α-CrB phase gradually increases, reaching the maximum value of 28 GPa at 90 GPa. The matching degree of toughness and hardness is the best, that is, the comprehensive mechanical properties of CrB are the best currently. When the pressure exceeds 90 GPa and the phase transition occurs, the hardness of β-CrB phase decreases significantly to as low as 9.3 GPa, and the *B/G* value increases to 3.9 currently, showing an obvious toughness characteristic.

4) The calculated results of mechanical anisotropy show that when the pressure exceeds 90 GPa to form a phase change, α-CrB phase has lower interatomic force and smaller bulk modulus. But in the crystal structure, the formation of chemical bonds network among atoms reduces the anisotropy of the bulk modulus, and thus, α-CrB phase has relatively high hardness and better comprehensive mechanical properties at 90 GPa.

References

1 Balasubramanian Karthik, Khare Sanjay V, Gall Daniel. *Acta Materialia*[J], 2018, 152 (1): 175

2 Beake Ben D, Harris Adrian J. *Vacuum*[J], 2019, 159: 17

3 Kovalev A I, Wainstein D L, Rashkovskiy A Y *et al. Vacuum*[J], 2009, 84 (1): 184

4 Puvaneswari S, Rajeswarapalanichamy R, Sudha Priyanga G. *Materials Chemistry and Physics*[J], 2015, 151: 149

5 Wang Shuanglun, Pan Yong, Lin Yuanhua *et al. Computational Materials Science*[J], 2018, 146: 18

6 Kapadia B M. *Journal of Heat Treating*[J], 1987, 5(1): 41

7 Nnamchi Paul S. *Materials & Design*[J], 2016, 108: 60

8 Xing W, Meng F, Yu R. *Sci Rep*[J], 2016, 6: 21 794

9 Zhang Jin, Oganov Artem R, Li Xinfeng *et al. Physical Review B*[J], 2017, 95 (2): 20 103

10 Liao P K, Spear K E. *Bulletin of Alloy Phase Diagrams*[J], 1986, 7: 232

11 Zhang Yanwen, Zhang Jidong. *Journal of Sichuan University, Natural Science Edition*[J], 2018, 55(4): 775

12 Li Xiaohong, Cui Hongling, Zhang Ruizhou. *Vacuum*[J], 2017, 145: 234

13 Wang Xia, Wang Lan, Pan Yong *et al. Vacuum*[J], 2017, 135: 121

14 Wang Yanchao, Lv Jian, Zhu Li *et al. Physical Review B*[J], 2010, 82 (9): 94 116

15 Wang Yanchao, Lv Jian, Zhu Li *et al. Computer Physics Communications*[J], 2012, 183(10): 2063

16 Coleman Jonathan N, Lotya Mustafa, O'Neill Arlene *et al. Science*[J], 2011, 331(6017): 568

17 Zhang Chunli, Yin Huanhuan, Han Min *et al. ACS Nano*[J], 2014, 8(4): 3761

18 Kresse Georg, Furthmüller Jürgen. *Physical Review B*[J], 1996, 54(16): 11 169

19 Perdew J P, Ruzsinszky A, Csonka G I *et al. Phys Rev Lett*[J], 2008, 100(13): 136 406

20 Sun Bo, Liu Shaojun, Zhu Wenjun. *Acta Phys Sin*[J], 2006, 55(12): 6589

21 Switendick A C, Morosin B. *AIP Conference Proceedings*[C]. American: American Institute of Physics, 1991: 205

22 Monkhorst Hendrik J, Pack James D. *Physical Review B*[J], 1976, 13(12): 5188

23 Chung D H, Buessem W R. *Journal of Applied Physics*[J], 1967, 38(6): 2535

24 Du Xiaodong, Ding Houfu, Xuan Tianpeng. *Chinese Journal of*

Nonferrous Metals[J], 2005, 15(12): 1980
25 Qin Ping, Gao Zhenbang, Liu Haidi *et al. Chinese Journal of Computational Physics*[J], 2019, 36(4): 491
26 Zhang Haiming, Dai Fuzhi, Xiang Huimin *et al. Journal of Materials Science & Technology*[J], 2019, 35(8): 1593
27 Wang Bing, Wang De Yu, Cheng Zhenxiang *et al. Chem Phys Chem*[J], 2013, 14(6): 1245
28 Born Max, Huang Kun, Lax M. *American Journal of Physics*[J], 1955, 23(7): 474
29 Chung D H, Buessem W R. *Journal of Applied Physics*[J], 1967, 38(5): 2010
30 Chong Xiaoyu, Jiang Yehua, Zhou Rong *et al. Journal of Alloys and compounds*[J], 2014, 610: 684
31 Li Runyue, Duan Yonghua. *Philosophical Magazine*[J], 2016, 96(10): 972
32 Xu Xuewen, Fu Kun, Li Lanlan *et al. Physica B: Condensed Matter*[J], 2013, 419: 105
33 Sun Yuan, Yang Ancang, Duan Yonghua *et al. International Journal of Refractory Metals and Hard Materials*[J], 2022, 103: 105 781
34 Pugh S F. *The London, Edinburgh, and Dublin Philosophical Magazine and Journal of Science*[J], 1954, 45(367): 823
35 Pettifor D G. *Materials Science and Technology*[J], 1992, 8(4): 345
36 Hearmon Roy Frederick Stanley, Maradudin Alexei A. *Physics Today*[J], 1961, 14(10): 48

不同压力下CrB的晶体结构、电子结构及力学性质的第一性原理研究

刘　飞，孙　伟，王　丽，贾　斌
(天津中德应用技术大学 机械工程学院，天津 300350)

摘　要：基于密度泛函理论第一性原理的方法，使用CALYPSO对CrB进行晶体进行结构搜索，并对搜索出的结构进行了电子结构的分析及力学性质的预测。结果表明，采用1倍分子式搜索出的2种结构中，α-CrB相为立方结构，空间群为Fm-3m（No. 225），β-CrB相为四方结构，空间群为P4/mmm（No. 123）。当压强超过90 GPa时，CrB将会发生结构相变，由α-CrB相转变为β-CrB相。声子谱的计算结果及力学稳定性的判据结果表明，α-CrB相及β-CrB相均具有动力学及力学稳定性。β-CrB相晶体中，B原子的s轨道、p轨道及Cr原子的d轨道发生杂化，形成共价键及离子键；α-CrB相晶体，Cr的d轨道和B的p轨道发生轨道杂化，形成了离子键。β-CrB相中态密度能量范围分布较大且峰值相对较低，能带色散较强，原子轨道相互作用较强。随着压力的增加，α-CrB相的硬度值逐渐升高，在90 GPa时达到最大值28 GPa，并且韧性和硬度的匹配程度最好，即此时材料的综合力学性能最好。当压力超过90 GPa发生相变后，β-CrB相的硬度值明显降低，低至9.3 GPa，此时B/G值增加至3.9，表现出明显的韧性特征。α-CrB相晶体虽然原子间作用力较低且体积模量较小，但是由于晶体内部原子之间形成了化学键网络，体积模量的各向异性相对较低，这是其具有较高硬度的主要原因。

关键词：第一性原理；晶体结构搜索；CrB；电子结构；超硬材料

作者简介：刘　飞，男，1987年生，博士，副教授，天津中德应用技术大学机械工程学院，天津 300350，电话：022-28776680，E-mail：lftjzd@126.com